Chinese Chemical Letters 31 (2020) 2614–2618

Contents lists available at ScienceDirect

Chinese Chemical Letters

journal homepage: www.elsevier.com/locate/cclet

Communication

Different non-radical oxidation processes of persulfate and peroxymonosulfate activation by nitrogen-doped mesoporous carbon

Hai-Bin Qiu, Pu-Can Guo, Li Yuan*, Guo-Ping Sheng*

CAS Key Laboratory of Urban Pollutant Conversion, Department of Applied Chemistry, University of Science and Technology of China, Hefei 230026, China

ARTICLE INFO

Article history:
Received 18 June 2020
Received in revised form 14 July 2020
Accepted 11 August 2020
Available online 13 August 2020

Keywords:
Nitrogen-doped mesoporous carbon
Persulfate
Peroxymonosulfate
Non-radical process
Electron transfer
Singlet oxygen formation

ABSTRACT

Activated persulfate oxidation is an emerging advanced oxidation process for organic pollutant degradation. Own to different molecular structures and oxidation potentials, persulfate (PDS) and peroxymonosulfate (PMS) may show different degradation performances due to various catalytic mechanisms even by the same catalysts. In this study, the nitrogen-doped mesoporous carbon (N-OMC) was applied to activate PDS and PMS for degrading a model organic pollutant phenol to reveal their activation mechanisms. Results show that both PDS and PMS could be efficiently activated by N-OMC. The degradation of phenol fitted well with *pseudo*-first-order kinetics, whose kinetic constants increased with the increase of pH, PDS/PMS dosage, and N-OMC dosage. Based on quenching experiments and electron spin resonance spin-trapping technique, the N-OMC was found to activate PDS and PMS *via* non-radical process of electron transfer and singlet oxygen formation, respectively, instead of the commonly observed radical process. This work will be useful to understand the activation processes of PDS and PMS, and benefit for the development of catalysts for pollutant degradation.

Hydroxyl radical ($^{\bullet}OH$) based advanced oxidation processes (AOPs), *e.g.*, Fenton reaction, are the most widely studied methods for the removal of organic contaminants from wastewater due to their excellent performances [1,2]. Compared with $^{\bullet}OH$, sulfate radical ($SO_4^{\bullet-}$) has compelling advantages with a higher oxidation potential and a longer half-life period [3]. Thus, the degradation of organic pollutants using $SO_4^{\bullet-}$, which can be generated by activating persulfate (PDS) or peroxymonosulfate (PMS), has raised increasing attention in recent years [4,5]. Various catalysts have been developed for PDS and PMS activation, including metal-based and non-metallic catalysts [6–9]. The non-metallic catalysts have recently attracted more attention because of their low cost, environment-friendly nature, and easy-to-design surface chemistry and pore structure [10]. In particular, the carbon nanotubes, graphene, diamond, activated carbon, and mesoporous carbon have been investigated in PDS or PMS activation for pollutant degradation [11–15]. However, the activation mechanisms of PDS or PMS obtained from previous studies sometimes are inconsistent and still need further exploration.

Generally, the activation of PDS and PMS is a radical oxidation process, but increasing evidence has also shown that it may be a non-radical oxidation process [13–17]. For example, some carbon-based catalysts, such as carbon nanotubes [13], mesoporous carbon [14], graphite diamond [15], benzoquinone [16], and quinone [17], have been found to activate PDS or PMS *via* non-radical process, including electron transfer process or singlet oxygen ($^1O_2$) formation. The non-radical oxidation process will have a higher reactivity to target pollutants in complex water matrices since the free radicals are more susceptible to solution pH, inorganic and organic matters in wastewater [9]. Furthermore, it is more effective to attack electron-rich pollutants *via* electron transfer and $^1O_2$ process [18,19]. Thus, the non-radical oxidation process broadens the application of PDS and PMS in wastewater treatment.

However, most previous studies only investigated the activation of sole PDS or PMS in the carbon-based catalyst systems. Since PDS and PMS have different molecular structures and oxidation potentials [4], it is speculated that they might also have different activation mechanisms by the same carbon-based catalysts. A few studies have observed that PDS and PMS had different performances in pollutant degradation after activation by the same catalyst [12,13]. Therefore, it is essential to reveal the differences in PDS and PMS activation mechanisms by using the same catalyst.

* Corresponding authors.
E-mail addresses: ly2016@ustc.edu.cn (L. Yuan), gpsheng@ustc.edu.cn (G.-P. Sheng).

https://doi.org/10.1016/j.cclet.2020.08.014
1001-8417/

In this work, the nitrogen-doped mesoporous carbon (N-OMC) was synthesized to activate PDS and PMS. Compared with other carbon materials, the mesoporous carbon owns a large surface area and unique mesoporous structure, which will favor the activation of PDS and PMS. Previous study indicated that the mesoporous carbon could enhance PDS activation *via* non-radical process, *e.g.*, electron transfer [14]. Doping N in graphitic carbon materials could generate active sites to mediate PMS for $^1O_2$ formation [20]. Thus, the mesoporous carbon functionalized with nitrogen doping is expected to activate PDS and PMS *via* different activation mechanisms. To verify this conjecture, phenol was used as a model organic pollutant. The effects of solution pH, PDS/PMS dosage, and N-OMC dosage on the degradation of phenol were assessed. The activation mechanisms for PDS and PMS were revealed to understand the different activation processes for PDS and PMS.

The N-OMC was synthesized as described previously [21,22]. Briefly, the silica template (SBA-15) was generated with pluronic 123 and ethyl orthosilicate as carbon and silicon sources, respectively. Afterward, 0.6 g SBA-15 was added to a mixture of aniline (0.5 mL) and 1 mol/L HCl (10 mL), and stirred for 15 min to obtain solution I. Ammonium persulfate (1.25 g) was dissolved in 2.23 mL 1 mol/L HCl to obtain solution II. The solution II was slowly added to the solution I and stirred for 20 h in an ice bath. The product was then dried at 60 °C, and the obtained solid powder was calcined and graphitized at 900 °C (heating rate 3 °C/min) for 4 h in N_2 atmosphere. The obtained product was desilicated twice in 2 mol/L NaOH solution at 80 °C, washed with distilled water, and dried under the ambient condition to generate N-OMC.

The transmission electron microscope (TEM) images of N-OMC were characterized using a TEM instrument (JEM-2011, JEOL Co., Japan). The surface chemistry and element chemical states of N-OMC were analyzed by X-ray photoelectron spectroscopy (XPS) (ESCALAB250, Thermo Fisher Inc. U. S. A.). The porosity and specific surface area were measured using the Brunauer-Emmett-Teller (BET) method with a Builder 4200 instrument (Tristar II 3020 M, Micromeritics Co., U. S. A.).

All degradation experiments of phenol by PDS or PMS activated by N-OMC were conducted in a 100 mL beaker at room temperature (23 ± 1 °C) and stirred at 800 rpm. The effects of N-OMC and PDS/PMS concentrations as well as solution pH on phenol degradation were investigated. The working solution was 60 mL containing 0.2 mmol/L phenol, 66.7 mmol/L phosphate buffer solution (PBS) (pH 4.5, 5.9, 7.0, 8.0, or 9.2), N-OMC (0.03, 0.07, or 0.1 g/L), and PDS/PMS (0.2, 0.5, or 1.0 mmol/L). Prior to PDS or PMS addition, the mixture of phenol and N-OMC in PBS was stirred for 10 min to reach adsorption equilibrium. The liquid samples were periodically collected and quickly filtered through 0.22 μm membrane filter. The concentration of phenol was detected using high-performance liquid chromatography (HPLC). All the degradation experiments were performed in duplicate.

The degradation of phenol was described using the *pseudo*-first-order kinetic model (Eq. 1).

$$\ln C_0/C_t = kt \quad (1)$$

where C_0 and C_t (mmol/L) were the concentrations of phenol at the initial time and time t (min), respectively; k (min^{-1}) was the *pseudo*-first-order kinetics constant obtained through Eq. 1.

To reveal the PDS and PMS activation mechanism by N-OMC for phenol degradation, quenching experiments and electron spin resonance (ESR) spin-trapping technique were performed to identify the potential reactive species involved during the activation process. In the quenching experiments, 400 mmol/L methanol, 180 mmol/L tert-butanol (TBA), or 10 mmol/L furfuryl alcohol (FFA) were used as the quenching agents. Methanol is a quenching agent for both $SO_4^{\bullet-}$ and $^{\bullet}OH$ with similar reaction rates ($k_{\bullet OH} = 9.7 \times 10^8\ m^{-1}s^{-1}$, $k_{SO_4^{\bullet-}} = 1.1 \times 10^7\ m^{-1}s^{-1}$) [23]. In contrast, TBA is regarded as $^{\bullet}OH$ quenching agent since its reaction rate with $^{\bullet}OH$ ($k_{\bullet OH} = 6 \times 10^8\ m^{-1}s^{-1}$) is much higher than that with $SO_4^{\bullet-}$ ($k_{SO_4^{\bullet-}} = 4 \times 10^5\ m^{-1}s^{-1}$) [23]. FFA is a quenching agent to determine whether $^1O_2$ was formed [24]. ESR measurements were conducted using an electron spin resonance instrument (JES-FA200, JEOL Co., Japan). The 5,5-dimethyl-1-pyrrolidine n-oxide (DMPO) was used as a spin trapping agent to detect $^{\bullet}OH$ and $SO_4^{\bullet-}$, and 2,2,6,6-tetramylpiperidine (TEMP) was applied to detect $^1O_2$ [25]. The linear sweep voltammetry (LSV) was employed to verify the electron transfer process using an electrochemical workstation (CHI660E, Chenhua Instrument Co., China) with a three-electrode cell. The N-OMC-modified glassy carbon electrode, Ag/AgCl, and Pt

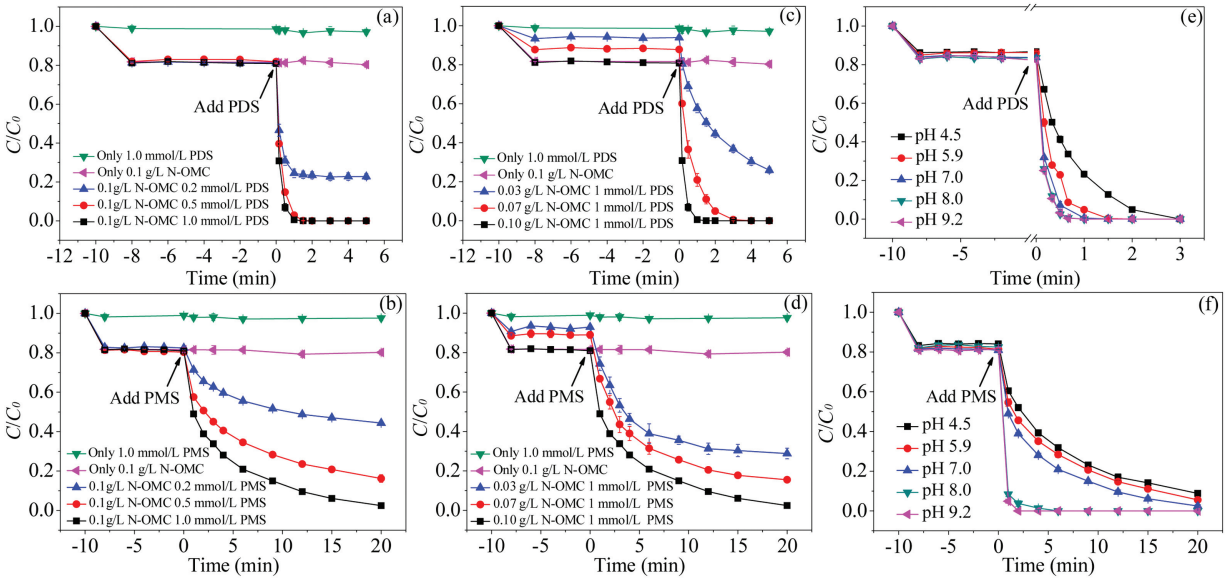

Fig. 1. Effects of PDS concentration (a), PMS concentration (b), N-OMC dosages (c, d), and solution pH (e, f) on the degradation of phenol in N-OMC/PDS or N-OMC/PMS system. Experimental condition: [phenol] = 0.2 mmol/L.

were used as the working, reference, and counter electrodes, respectively. The LSV was measured at a scan rate of 0.5 mV/s in 66.7 mmol/L phosphate buffer solution (pH 7.0).

The concentration of phenol was determined by Agilent 1260 Infinity HPLC instrument equipped with Agilent Eclipse Plus C18 chromatographic column (4.6 mm ID × 250 mm, 5 μm particle size) and a diode array detector (set at 210 nm). The mobile phase was a mixture of acetonitrile and water (3:7, v/v) at a flow rate of 0.8 mL/min. The variations of PDS and PMS concentrations in the degradation process were detected by UV-2600 spectrophotometer (Shimadzu, Japan) at 352 nm based on the iodometric titration method [14]. To reveal the mineralization of phenol by PDS and PMS activated by N-OMC, total organic carbon (TOC) concentration during phenol degradation was determined by a TOC analyzer (multiN/C 2100, Analytik Jena, Germany).

The BET surface area of N-OMC was 1021.3 m^2/g. Based on the TEM image (Fig. S1a in Supporting information), the N-OMC had a relatively clear pore structure with striated arrangement, which was similar to the morphology of other mesoporous carbon materials reported previously [14]. The XPS spectrum (Fig. S1b in Supporting information) demonstrates that N element was successfully doped into the N-OMC. The N-OMC had a hysteretic curve in the P/P_0 range of 0.7–0.8 with an average pore size of 5.6 nm based on the isothermal curve (Fig. S1c in Supporting information) and adsorption curve (Fig. S1d in Supporting information).

As shown in Fig. 1, the phenol could not be removed in the control experiments without N-OMC addition, demonstrating that sole PDS or PMS could not degrade phenol. About 20% phenol was removed by 0.1 g/L N-OMC in the absence of PDS or PMS, which was owed to the adsorption by N-OMC. After PDS or PMS was dosed, the removal efficiencies increased sharply to 77%–100% for PDS system (Fig. 1a) and 56%–98% for PMS system (Fig. 1b). Given that N-OMC/PDS system could degrade phenol more efficiently, the mineralization of phenol by N-OMC/PDS was further assessed. 18% of TOC could be removed by N-OMC (0.1 g/L) adsorption (Fig. S2 in Supporting information). In the N-OMC/PDS system, the TOC content of phenol was removed by 51% (including adsorption) within 5 min (Fig. S2), indicating that the N-OMC/PDS system could efficiently mineralize/adsorb phenol.

The dosages of PDS or PMS could influence the phenol degradation (Figs. 1a and b). The degradation kinetics constants k (Table S1 in Supporting information) increased from 1.59 min^{-1} to 5.58 min^{-1} for PDS and from 0.0313 min^{-1} to 0.232 min^{-1} for PMS with the increase of their concentrations from 0.2 mmol/L to 1.0 mmol/L, respectively. Increasing N-OMC dosage also could promote phenol degradation (Figs. 1c and d). The degradation kinetics constant k (Table S1) increased from 0.285 min^{-1} to 5.58 min^{-1} for PDS and from 0.0812 min^{-1} to 0.232 min^{-1} for PMS with the increase of N-OMC dosages from 0.03 g/L to 0.10 g/L, respectively. Furthermore, under the same conditions, the degradation kinetics constants of phenol by PDS were 3.5–50.8 folds higher compared with those by PMS, indicating PDS was more efficient for phenol degradation activated by N-OMC.

The effect of solution pH on N-OMC activation for phenol degradation was shown in Figs. 1e and f. The degradation kinetics constant k (Table S1) increased from 1.40 min^{-1} to 6.63 min^{-1} with pH increased from 4.5 to 8.0, and then remained constant with pH further increased to 9.2 in the N-OMC/PDS system (Fig. 1e). In contrast, the degradation kinetics constant k remained relatively constant in pH range of 4.5–7.0, and then increased remarkably with pH further increase to 9.2 in the N-OMC/PMS system (Fig. 1f, Table S1). In the N-OMC/PDS system, the degradation kinetics constant of phenol increased with the increase of pH, which was attributed to that PDS could be activated easier at alkaline pH [14]. In the N-OMC/PMS system, the enhanced removal of phenol at pH > 8.0 was probably because the phenolic compounds could be degraded by PMS alone *via* the singlet oxygen pathway at alkaline pH (*e.g.*, pH 8 or 9) [26,27]. Thus, the higher removal of phenol in the N-OMC/PMS system at pH > 8.0 might be attributed to the synergistic effects of both alkaline and catalyst activation. The different trends of phenol degradation with pH implied that the activation of N-OMC for PDS and PMS might be different.

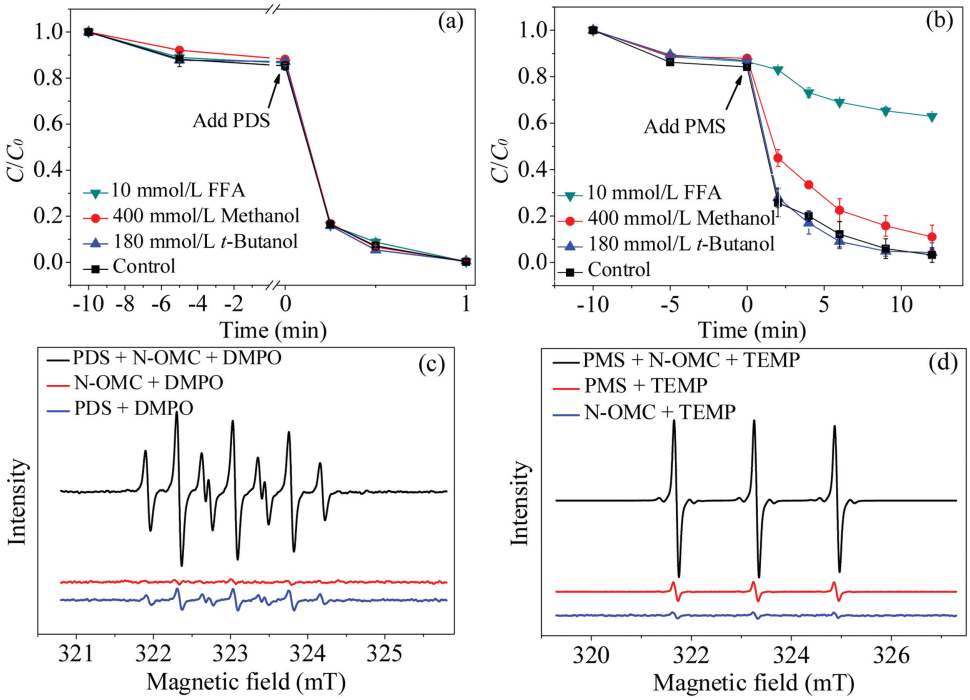

Fig. 2. Effects of MeOH (400 mmol/L), TBA (180 mmol/L), and FFA (10 mmol/L) addition on the degradation of phenol in (a) N-OMC/PDS or (b) N-OMC/PMS systems. ESR spectra of (c) PDS and (d) PMS activated by N-OMC. Experimental conditions: [phenol] = 0.2 mmol/L, [N-OMC] = 0.1 g/L, [PDS or PMS] = 1 mmol/L, and pH 7.0.

Generally, the main mechanisms of activating PDS or PMS for pollutant degradation include radical (*e.g.*, generation of $SO_4^{\bullet-}$ and $^{\bullet}OH$) and non-radical (*e.g.*, electron transfer or $^1O_2$ generation) oxidation processes. Quenching experiments were carried out to determine the possible reactive species involved in phenol degradation. As shown in Fig. 2a, the degradation of phenol by PDS was not inhibited with addition of methanol, TBA, or FFA. Their degradation kinetics constants (6.23–6.61 min^{-1}, Fig. S3 in Supporting information) of phenol were similar to that of the control group, indicating that PDS could not be activated by N-OMC to generate $SO_4^{\bullet-}$, $^{\bullet}OH$, or $^1O_2$. It was speculated that electron transfer might be the major activation mechanism of PDS by N-OMC. In contrast, in the N-OMC/PMS system, FFA addition greatly inhibited phenol degradation with the degradation kinetics constant decreased from 0.431 min^{-1} to 0.029 min^{-1} (Fig. 2b). Since PMS could be depleted by FFA, in order to prove that most FFA was involved in quenching $^1O_2$ rather than depleting PMS, the degradation of PMS in the presence of 10 mmol/L FFA was determined. Only about 20% of PMS was removed after 20 min at 10 mmol/L FFA (Fig. S4 in Supporting information). Meanwhile, FFA can inhibit the degradation kinetics constant of phenol by 93% in the quenching experiment (Fig. 2b). Thus, most FFA was involved in $^1O_2$ quenching rather than PMS depletion. The TBA had little inhibited effect on phenol degradation (Fig. 2b). Moreover, methanol slightly inhibited phenol degradation, which might be due to that methanol could react with PMS slightly [28]. These results indicated that PMS could be activated by N-OMC mainly to generate $^1O_2$ instead of $SO_4^{\bullet-}$ and $^{\bullet}OH$. Thus, the activation mechanisms of PDS and PMS by N-OMC were different.

To confirm the phenomenon observed in the quenching experiments, DMPO (capturing $SO_4^{\bullet-}$ and $^{\bullet}OH$) and TEMP (capturing $^1O_2$) were used as spin-trapping agents for ESR detection. As shown in Fig. 2c, no characteristic peaks of DMPO–OH (hyperfine splitting of $\alpha_H = \alpha_N = 14.9$ G) or DMPO-SO_4 (hyperfine splitting of $\alpha_H = 9.6$ G, $\alpha_H = 1.48$ G, $\alpha_N = 0.78$ G, and $\alpha_N = 13.2$ G) [24] were observed in the N-OMC/PDS system, confirming that $SO_4^{\bullet-}$ and $^{\bullet}OH$ were not generated. Instead, six characteristic peaks of DMPOX [29], which was oxidized derivative of DMPO, was observed in the N-OMC/PDS system. This proved that $SO_4^{\bullet-}$ and $^{\bullet}OH$ were not produced in N-OMC/PDS system. Similarly, the characteristic peaks of DMPOX were also observed in the N-OMC/PMS system, proving that $SO_4^{\bullet-}$ and $^{\bullet}OH$ were not generated in the N-OMC/PMS system (Fig. S5 in Supporting information). Meanwhile, some characteristic peaks generated by the reaction of TEMP and $^1O_2$ (hyperfine splitting of $\alpha_N = \alpha_N = \alpha_N = 16.9$ G) [30] were observed in the N-OMC/PMS system (Fig. 2d), confirming that N-OMC could activate PMS *via* $^1O_2$ generation.

The concentrations of PDS and PMS during the reaction process were also monitored. As shown in Fig. 3a, the PDS content remained unchanged in the phenol solution in the absence of N-OMC, while it decreased by about 10% in the first 10 min after N-OMC addition and then remained relatively level in the absence of phenol. The decrease in PDS concentration was probably due to its adsorption onto N-OMC. This result indicates that N-OMC alone could not catalyze PDS decomposition in the absence of phenol, which was similar to the previous study [12]. In contrast, in the presence of phenol and N-OMC, PDS content decreased continuously with the reaction time. Our results have indicated that the degradation of phenol in the N-OMC/PDS system was an electron transfer process without radical generation (*e.g.*, $SO_4^{\bullet-}$). Specifically, N-OMC acted as an electron transport channel, transporting electrons from the electron donor (phenol) to the electron acceptor (PDS). During this process, PDS gained electrons to form SO_4^{2-} and phenol lost electrons to be oxidized. Thus, without phenol, PDS could not be decomposed and its concentration remained unchanged with time.

The LSV was employed to further confirm the electron transfer mechanism. The current increase was negligible with the addition of PDS or phenol alone. However, the current increased significantly when PDS and phenol were added simultaneously, verifying the presence of the electron transfer in the N-OMC/PDS system (Fig. S6 in Supporting information). However, the PMS content decreased continuously with the reaction time after N-OMC addition with or without phenol (Fig. 3b). Thus, PMS would be activated by N-OMC alone to produced $^1O_2$ rather than $SO_4^{\bullet-}$ and $^{\bullet}OH$ for phenol degradation.

This study observed two different catalytic mechanisms, *i.e.*, electron transfer and $^1O_2$ formation processes, for PDS and PMS activation by N-OMC, respectively. Although both PDS and PMS are persulphate oxides with O—O bonds, they are quite different in molecular structure. The PDS is symmetric and less vulnerable compared with PMS. Meanwhile, PDS has longer O—O bonds, which are more likely to break down than PMS [13]. Moreover, they have different oxidation potentials (*i.e.*, PDS: E^0 ($S_2O_8^{2-}/SO_4^{2-}$) = 1.96 V, *vs.* NHE; PMS: E^0 (HSO_5^-/SO_4^{2-}) = 1.75 V, *vs.* NHE) [12]. Thus, the different mechanisms might be attributed to their different molecular structures and oxidation potentials of PDS and PMS, and more works are needed to investigate the difference in PDS and PMS activation mechanisms.

In addition, the underlying mechanisms for different activation processes of PDS and PMS by N-OMC could be attributed to N doping, which probably altered the functional groups in OMC and thus resulted in different activation mechanisms. It has been reported that the N dopping could possess high electron-transfer capacity and thus facilitate the electron transport between

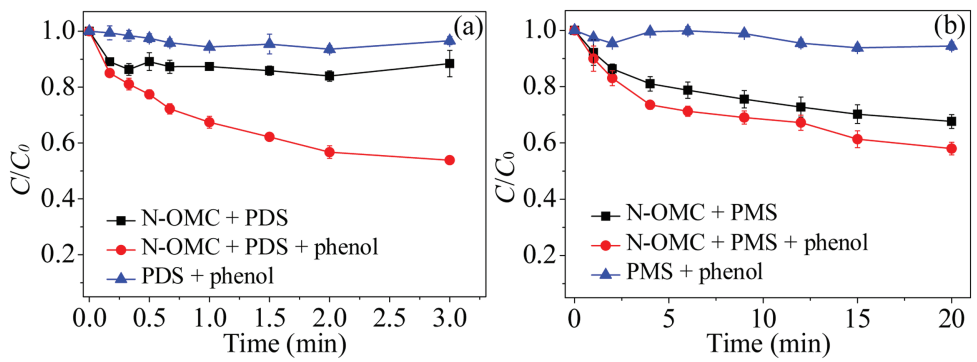

Fig. 3. Variations of (a) PDS and (b) PMS concentrations during phenol degradation. Experimental conditions: [phenol] = 0.2 mmol/L, [N-OMC] = 0.1 g/L, [PDS or PMS] = 1 mmol/L, and pH 7.0.

carbon-based catalyst and PMS [11]. In particular, the graphitic N could activate PMS to produce $^1O_2$ [20]. In the future, more analysis and research should be carried out to prove the role of N in the activation process of N-OMC/PDS and N-OMC/PMS systems. However, different phenomena have been observed in the literature of N doping catalyst. For example, the activation mechanism of PDS and PMS remained as electron transfer process by carbon nanotubes even after N doping [13]. These indicate that structures of carbon materials could influence the activation process for PDS and PMS activation. Future research is required to explore the relationship of the activation mechanism with the surface structure and element contents of carbon-based catalysts for PDS and PMS.

Moreover, the degradation efficiencies *via* electron transfer and $^1O_2$ formation processes generally vary significantly among different pollutants [31–33]. For example, due to the electrophilic nature, $^1O_2$ can selectively oxidize organic pollutants, such as pharmaceuticals and endocrine disruptor chemicals, in complex water matrices [31,32], thus PMS activated by N-OMC could be applied for the degradation of these pollutants. The electron-rich organic contaminants (*e.g.*, phenol, trichloroethylene, and chlorophenols) could be easily degraded *via* the electron transfer pathway [19,33], and thus PDS activated by N-OMC would be more effective to remove these pollutants. This would provide a reference for the application of PDS/PMS in water and wastewater treatment based on the properties of target pollutants.

In summary, PDS and PMS could be efficiently activated by N-OMC for phenol degradation *via* two different non-radical processes, *i.e.*, electron transfer and $^1O_2$ formation. The degradation phenol by PDS and PMS was dependent on pH, PDS/PMS dosage, and N-OMC dosage. The N-OMC activated PDS/PMS system *via* non-radical process can serve as a promising treatment technology for organic pollutant removal.

Declaration of competing interest

The authors declare that they have no known competing financial interests or personal relationships that could have appeared to influence the work reported in this paper.

Acknowledgments

The authors wish to thank the National Key R&D Program of China (No. 2019YFC0408502) and the National Natural Science Foundation of China (NSFC) (Nos. 51825804, 51821006) for the support of this study.

Appendix A. Supplementary data

Supplementary material related to this article can be found, in the online version, at doi:https://doi.org/10.1016/j.cclet.2020.08.014.

References

[1] B.C. Hodges, E.L. Cates, J.H. Kim, Nat. Nanotechnol. 13 (2018) 642–650.
[2] D.B. Miklos, C. Remy, M. Jekel, et al., Water Res. 139 (2018) 118–131.
[3] A. Tsitonaki, B. Petri, M. Crimi, et al., Crit. Rev. Environ. Sci. Technol. 40 (2010) 55–91.
[4] J. Wang, S. Wang, Chem. Eng. J. 334 (2018) 1502–1517.
[5] C.D. Qi, G. Yu, J. Huang, et al., Chem. Eng. J. 353 (2018) 490–498.
[6] H. Zhang, Q. Ji, L. Lai, G. Yao, B. Lai, Chin. Chem. Lett. 30 (2019) 1129–1132.
[7] M. Ma, L. Chen, J. Zhao, et al., Chin. Chem. Lett. 30 (2019) 2191–2195.
[8] L.D. Lai, H.Y. Zhou, B. Lai, Chem. Eng. J. 349 (2018) 633–645.
[9] E.T. Yun, H.Y. Yoo, H. Bae, H.I. Kim, J. Lee, Environ. Sci. Technol. 51 (2017) 10090–10099.
[10] L. Liu, Y.P. Zhu, M. Su, et al., ChemCatChem 7 (2015) 11878–11886.
[11] X. Duan, H. Sun, Y. Wang, J. Kang, S. Wang, ACS Catal. 5 (2014) 553–559.
[12] H. Lee, H.J. Lee, J. Jeong, et al., Chem. Eng. J. 266 (2015) 28–33.
[13] W. Ren, G. Nie, P. Zhou, et al., Environ. Sci. Technol. 54 (2020) 6438–6447.
[14] L. Tang, Y. Liu, J. Wang, et al., Appl. Catal. B: Environ. 231 (2018) 1–10.
[15] H. Lee, H.I. Kim, S. Weon, et al., Environ. Sci. Technol. 50 (2016) 10134–10142.
[16] Y. Zhou, J. Jiang, Y. Gao, et al., Environ. Sci. Technol. 49 (2015) 12941–12950.
[17] G. Fang, J. Gao, D.D. Dionysiou, C. Liu, D. Zhou, Environ. Sci. Technol. 47 (2013) 4605–4611.
[18] P. Hu, H. Su, Z. Chen, et al., Environ. Sci. Technol. 51 (2017) 11288–11296.
[19] S.H. Ho, Y.D. Chen, R. Li, et al., Water Res. 159 (2019) 77–86.
[20] Y. Gao, Z. Chen, Y. Zhu, T. Li, C. Hu, Environ. Sci. Technol. 54 (2020) 1232–1241.
[21] D. Zhao, J. Feng, Q. Huo, et al., Science 279 (1997) 548–552.
[22] R. Silva, A.V. Biradar, L. Fabris, T. Asefa, J. Phys. Chem. C 115 (2011) 22810–22817.
[23] G.V. Buxton, C.L. Greenstock, W.P. Helman, A.B. Ross, J. Phys. Chem. Ref. Data 17 (1988) 513–886.
[24] H.E. Gsponer, C.M. Previtali, N.A. García, Toxicol. Environ. Chem. 16 (1987) 23–37.
[25] J. Moan, E. Wold, Nature 279 (1979) 450–451.
[26] C.D. Qi, X.T. Liu, J. Ma, et al., Chemosphere 151 (2016) 280–288.
[27] Y. Yang, G. Banerjee, G.W. Brudvig, J.H. Kim, J.J. Pignatello, Environ. Sci. Technol. 52 (2018) 5911–5919.
[28] W. Zhu, W.T. Ford, J. Org. Chem. 56 (1991) 7022–7026.
[29] A. Lawrence, C.M. Jones, P. Wardman, M.J. Burkitt, J. Biol. Chem. 278 (2003) 29410–29419.
[30] B. Song, G. Wang, M. Tan, J. Yuan, J. Am. Chem. Soc. 128 (2006) 13442–13450.
[31] H. Kim, W. Kim, Y. Mackeyev, et al., Environ. Sci. Technol. 46 (2012) 9606–9613.
[32] J. Lee, S. Hong, Y. Mackeyev, et al., Environ. Sci. Technol. 45 (2011) 10598–10604.
[33] T. Zhang, Y. Chen, Y. Wang, et al., Environ. Sci. Technol. 48 (2014) 5868–5875.